Mode Coupling by a Longitudinal Slot for a Class of Planar Waveguiding Structures: Part II—Applications

PERRY F. WILSON, MEMBER, IEEE, AND DAVID C. CHANG, FELLOW, IEEE

Abstract—**Coupling between two parallel-plate waveguides is investigated. Mutual excitation is due to a longitudinal slot in a common plate. The introduction of reflecting boundaries parallel to the slot allows one to model a number of planar waveguiding structures featuring a common coupling mechanism. Part II of this paper presents specific examples of the above approach along with numerical results. Examples include a rectangular coaxial transmission line, broadwall-coupled rectangular waveguides, coupled microstrips, and coupled microstrip and rectangular waveguide.**

I. Introduction

PART I OF THIS PAPER [1] analyzed the scattering due to a slot between loaded parallel-plate waveguides. The solution to this canonical problem can be used to determine the modal properties of a class of planar waveguiding structures featuring this common slot coupling mechanism. Rather than attempt a full modal description, the investigation presented in Part I considered LSM-type modes with lateral resonances only. More general results are certainly obtainable, but at the expense of the simple, closed-form modal equations developed here. Our present scope should cover the dominant TE or quasi-TEM mode as well as other low-order TE-type modes.

Part II of this two-part paper presents four specific applications of the modal equations derived in Part I. Considered are: 1) a rectangular coaxial transmission line (RCTL), which is a form of shielded stripline; 2) symmetric broadwall-coupled rectangular waveguides, a type of shielded slotline; 3) coupled microstrips; and 4) coupled microstrip and rectangular waveguides. In the first two examples, the RCTL and coupled rectangular waveguides, we consider the propagation of low-order TE-type modes. Each of these geometries has been analyzed elsewhere and a comparison of results serves to demonstrate the accuracy and limitations of the two modal equations developed in Part I. The second pair of examples involving microstrip coupling are more original. These latter two geometries will be viewed as directional couplers and the discussion oriented toward how efficiently they couple power between guides.

Manuscript received February 28, 1985; revised June 5, 1985. This work, performed at the University of Colorado, was supported in part by the National Bureau of Standards and monitored by Drs. M. T. Ma and M. Kanda.

P. F. Wilson is with the Electromagnetic Fields Division, National Bureau of Standards, Boulder, CO 80303.

D. C. Chang is with the Department of Electrical and Computer Engineering, University of Colorado, Boulder, CO 80309.

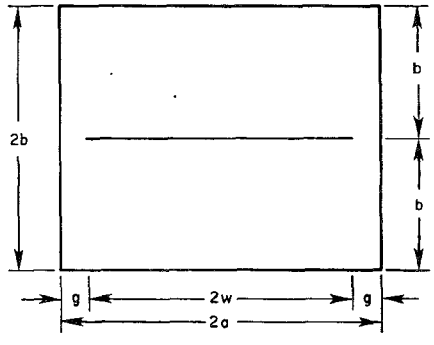

Fig. 1. Rectangular coaxial transmission line.

We conclude with a section on possible additional applications as well as desirable extensions. In fact, the emphasis of Part II is not simply on the specific examples mentioned above. Rather, a more important goal is to demonstrate the flexibility and range with which the basic scattering solution presented in Part I may be employed.

II. Higher Order Modes in a RCTL

The RCTL cross section, as depicted in Fig. 1, consists of an outer conductor of aspect ratio $2a \times 2b$ with an inner strip of width $2w$ offset from the side walls by gaps g, and displaced from the ceiling and floor by b_1 and b_2, respectively. The RCTL has been well studied [2]–[5] because of its application in TEM-cell measurement devices and in microwave circuits. The primary emphasis of these investigations is to determine the RECTL's transmission-line characteristics. However, because the appearance of higher order modes typically limits the usable TEM-mode frequency range, the cutoff frequencies of the initial higher order modes [6]–[10], as well as methods for extending the upper frequency limit [11], [12], are of interest.

Referring to our basic slotted cross section [1, Fig. 4], a RCTL may be reproduced as follows. If the slot is centrally located with respect to the scattering walls (i.e., $\text{off}_1 = \text{off}_2 = 0$), then the vertical electric-field component E_y will be either symmetric or antisymmetric about the slot. In the dominant logarithmic coupling case, E_y will be antisymmetric about the slot center ($x = 0$), which is equivalent to the presence of a vertical electric wall. Placing reflecting

0018-9480/85/1000-0988$01.00 ©1985 IEEE

walls at $x = \pm a$ above and below the slot ($l_1 = l_2 = a$) effectively creates a pair of RCTL's imaged about $x = 0$. Assuming the RCTL is empty ($\epsilon_{r1} = \epsilon_{r2} = 1$) implies that $E_z = 0$ [1, eq. (17)]; thus, we are considering the TE_{mn} modes. If we choose magnetic walls at $x = \pm a$, then E_y will be evenly distributed about the septum center, implying a m-odd TE_{mn} mode. Alternately, electric walls at $x = \pm a$ yield the m-even TE_{mn} modes.

The modal equations derived in Part I may be used to determine either the normalized propagation constant α, or setting $\alpha = 0$, the cutoff frequency, wavelength, etc. Consider an unloaded cell (as above), with a centrally located septum ($b_1 = b_2 = b$). Then the reduced, logarithmic gap-dependent modal equation [1, eq. (39)] is appropriate. Letting $d_1 = d_2 = b$, $l_1 = l_2 = a$, $\text{off}_1 = \text{off}_2 = 0$, and $\chi_j(\alpha) = (m+1)\pi$ consistent with our m-even/odd discussion above, yields the following modal equation:

$$\beta_0 \sin^2\phi \left\{ \frac{\pi}{k_0 b} \tan\frac{\phi}{2} + 2\beta_0 \left[\ln\left(\frac{2b}{\pi g}\right) + R \right] \right\} = 0$$

$$R = \sum_{m=1}^{\infty} \left[\frac{\pi}{k_0 \gamma_m b} - \frac{1}{m} \right]$$

$$\phi = 2k_0\beta_0 a - (m+1)\pi \qquad (1)$$

where β_0 and γ_m are defined in Part I. There are three separate solutions implied by (1). If we set $\beta_0 = 0$, then we find $\alpha = 1$, which is the normalized propagation constant for the TEM mode. Setting $\sin^2\phi = 0$ determines the TE_{m0} m odes. Note that the TE_{m0} modes are unaffected by the gap (see [1, eq. (17)] and note that $E_1^+ = E_2^+$, $E_1^- = E_2^-$, etc.; thus, the gap fields are unexcited). Finally, the expression in brackets determines the TE_{m1} modes. Our approximation assumes the E_y is essentially independent of y; therefore, the TE_{mn} modes for $n > 1$ cannot be analyzed via the present expressions. If we note that

$$\tan\frac{\phi}{2} = \begin{cases} -\cot k_0\beta_0 a, & m\text{-even} \\ \tan k_0\beta_0 a, & m\text{-odd} \end{cases} \qquad (2)$$

and let $u = k_0\beta_0 a$, then the TE_{m1} modal equations become

$$u \tan u = \frac{\pi}{2}\frac{b}{a}\left\{ \ln\left(\frac{2b}{\pi g}\right) + R \right\}^{-1}, \qquad m\text{-even} \quad (3a)$$

$$\frac{1}{u}\tan u = \frac{2}{\pi}\frac{b}{a}\left\{ \ln\left(\frac{2b}{\pi g}\right) + R \right\}, \qquad m\text{-odd}. \quad (3b)$$

These equations can be readily solved. In fact, if we note that for $k_0 b$ small, the remainder series may be approximated as follows:

$$R \approx \frac{1}{2}\left(\frac{u}{\pi}\frac{b}{a}\right)^2 \zeta(3) \qquad (4)$$

then (3) is easily solved on a hand calculator. For example, Hill [13] has published data for the cutoff frequencies of the first few higher order modes in an RCTL of dimensions $a = b = 1.5$ m and $g = 0.26$ m. He finds that f_c for the TE_{01} mode is approximately 29.0 MHz, while for the TE_{11} mode, $f_c \approx 63.5$ MHz. As $g/b \to 0$, (30) behaves like $u \tan u = 0$, which has a first solution, $u = 0$. Thus, as is known, the cutoff frequency of the TE_{01} mode goes to zero as the gap vanishes. Neglecting R, which has a u^2 dependence, (3a) yields $u \approx 0.9198$ or $f_c \approx 29.3$ MHz, which compares well with Hill's value. Similarly, (3b) degenerates to $\tan u/u = \infty$ as $g/b \to 0$, which has an initial solution of $u = \pi/2$, which as expected is the solution for the TE_{10} mode. If we now include the remainder term (4) then (3b) yields $u \approx 2.033$, or $f_c \approx 64.7$ MHz, again in good agreement with Hill's data. Note that (3) could be used to examine additional modes. For example, the next solution for (3a) should be for $u > \pi$ corresponding to the TE_{21} mode. However, the accuracy is expected to decrease since the condition that the gap be electrically narrow will weaken.

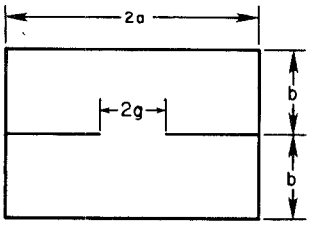

Fig. 2. Shielded slotline.

Variations on the above RCTL structure can be studied via the asymmetric modal equation. For example, the inner conductor could be vertically offset to create a larger chamber. In terms of TEM-cell usage, this would allow larger pieces of equipment to be tested. One or both of the chambers could be loaded with dielectric. This would remove the plane-wave environment necessary for TEM-cell applications; however, viewed as a shielded stripline, this structure may have microwave device potential. The interference between the even–odd TE_{10} modes could also be used as the basis for a rectangular waveguide directional coupler.

A structure related to the RCTL just discussed is depicted in Fig. 2, namely, a pair of slot-coupled rectangular waveguides or shielded slotline. For the central slot location shown, E_y will be either laterally anti-symmetric, in which case the previous equations again apply (TE_{m1} modes, m-even), or laterally symmetric (TE_{m1} modes, m-odd). The TE_{mn} modes, n-even, will again be unaffected by the gap. For the TE_{m1} modes, m-odd, the symmetric mode equation (41) of Part I applies

$$1 - \Gamma - 4\rho\Gamma = 0 \qquad (5)$$

where $d_1 = d_2 = b$, $l_1 = l_2 = a$, and $\chi(\alpha) = m\pi$ (m-odd) corresponding to an electric wall. Up to terms of the order $(k_0 g)^2$, (5) may be inverted directly with the result that

$$\alpha = 1 - \left(\frac{m\pi}{2k_0 a}\right)^2 - \frac{m^2\pi^3 (k_0 g)^2}{8(k_0 a)^2 k_0 d}. \qquad (6)$$

The first two terms represent the unperturbed ($g = 0$) TE_{m0} normalized propagation constant while the third $[k_0 g)^2$-dependent term gives the gap affect. Equation (6) has been verified elsewhere for the case $m = 1$ based on a variational formulation [14]. If the slot were to be used to

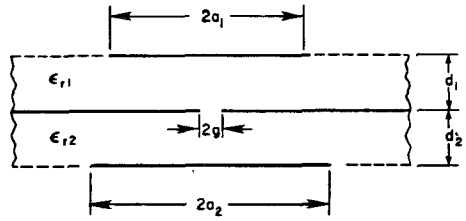

Fig. 3. Coupled microstrips.

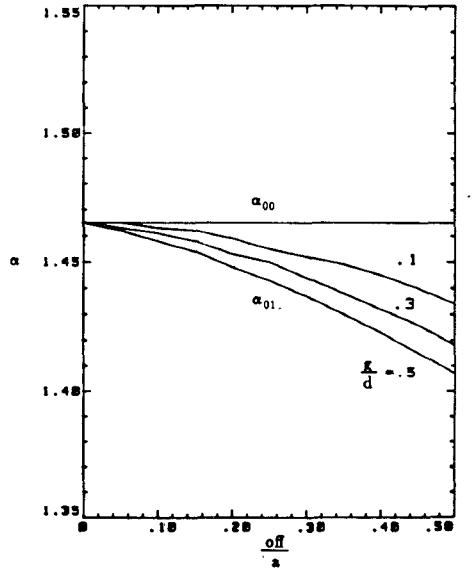

Fig. 4. The variation of the propagation constants α_{00} and α_{01} versus slot offset for coupled identical microstrips ($\epsilon_r = 2.56, k_0 a = 0.2, k_0 d = 0.1$).

couple two rectangular waveguides based on the interference between TE_{10} and TE_{11} modes, then the coupling length would have a $(k_0 g)^{-2}$ dependence [15], which is assumed to be large. This again demonstrates that broadwall coupling via longitudinal slots is more efficient if the slot is offset to introduce the logarithmically dependent gap fields.

III. Coupled Microstrips

The previous two examples have featured structures analyzed elsewhere and serve to demonstrate the usefulness of the two modal equations derived in Part I. We now consider a more novel application, namely, a pair of coupled microstrips as depicted in Fig. 3. The microstrips are allowed to have arbitrary loading ϵ_{rj}, thickness d_j, and width $2a_j$.

Although the slot is depicted as centrally located, our previous discussion indicates that the slot should be offset to increase the interaction between the guides if this configuration is to be used to couple power between microstrips. Thus, the asymmetric modal equation is appropriate. As an example, consider two identical microstrips ($\epsilon_{r1} = \epsilon_{r2} = \epsilon_r$, etc.), equally offset, with $\epsilon_r = 2.56$, $k_0 a = 0.2$, and $k_0 d = 0.1$. The phase change $\chi(\alpha)$ at the microstrip reflecting boundaries ($x = \pm a$) appears in the literature [16], [17]. Fig. 4 shows the variation of α versus slot offset and width

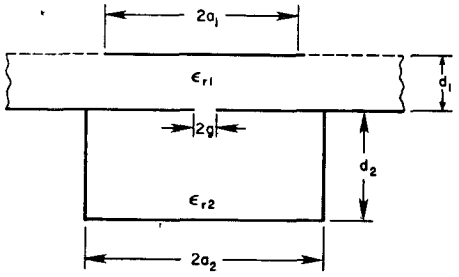

Fig. 5. Coupled microstrip and rectangular waveguide.

for the quasi-TEM mode (α_{00}: E_y aligned in the two microstrips) and the TE_{01} mode (α_{01}: E_y opposed in the two microstrips). As expected, α_{00} is unaffected by the gap and equals the propagation constant of the quasi-TEM mode in each guide. The TE_{01} mode is increasingly perturbed as either the slot offset (off/a) or width (g/d) is increased. However, the perturbation is slight due to the fact that E_y is relatively uniform across the slot (x-variation). The small difference between α_{00} and α_{01} implies that the large coupling lengths would be necessary to achieve maximal power between the two microstrips if the interference of the quasi-TEM mode (α_{00}) and TE_{01} mode (α_{01}) is to be the coupling mechanism. Specifically, $k_0 L = \pi(\alpha_{00} - \alpha_{01})^{-1}$; thus, at the extremes of the present example (off/a $= 0.5$, $g/d = 0.5$), we still have $L \approx 8.7\lambda_0$, where L is the coupling length and λ_0 is the free-space wavelength. If coupling between dissimilar microstrips is desired, then the slot effect should be more pronounced, thereby reducing coupling lengths; however, full-power transfer would no longer be expected.

IV. Slot Coupled Microstrip and Rectangular Waveguide

All of the previous examples have featured coupling between generically similar guides, greatly aiding in their analysis via conventional approaches. We now will consider coupling between two very different guides, namely, a microstrip and a rectangular waveguide as shown in Fig. 5. The pertinent dimensions are labeled and the guides are allowed to have arbitrary dielectric loading. Although the slot is depicted as centrally located, it will be allowed to be offset.

Coupling power between these two types of waveguides has been the topic of a number of studies. As the operating frequency of a microstrip increases, conventional waveguide–coax–stripline transitions become physically more difficult, as well as costly. Thus, a mode launching technique compatible with planar technology is desirable.

Various alternatives to coax feeding have been suggested. Knerr [18] proposes a broad-band coupler based on inserting the stripline perpendicularly into the rectangular waveguide broadwall. He then models the junction as a coupled tuned circuit and applies well-known results to optimize the design. This approach yields good bandwidth properties but is physically somewhat awkward. Other problems with direct insertion schemes have been discussed by Wild [19]. A primary concern is the spurious radiation

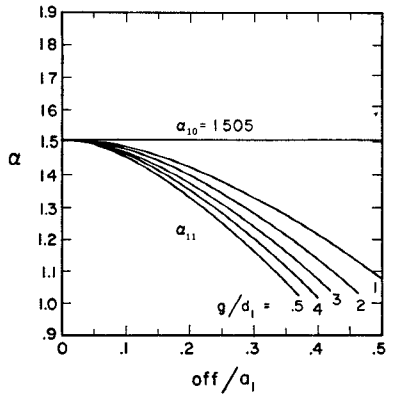

Fig. 6. The variation of the propagation constants α_{10} and α_{11} versus slot offset for coupled microstrip and rectangular waveguide ($\epsilon_{r1} = 2.56, \epsilon_{r2} = 9.0, k_0 a_1 = 0.5, k_0 a_2 = 0.61, k_0 d_1 = 0.25, k_0 d_2 = 0.5$).

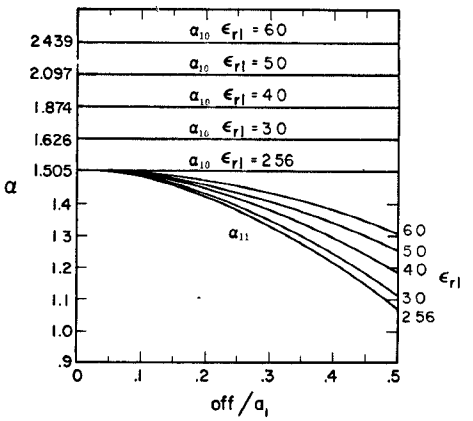

Fig. 7. The variation of the propagation constants α_{10} and α_{11} versus slot offset for coupled microstrip and rectangular waveguide ($\epsilon_{r2} = 9.0, k_0 a_1 = 0.5, k_0 a_2 = 0.61, k_0 d_1 = 0.25, k_0 d_2 = 0.5, g/d_1 = 0.1$).

created by network discontinuities, a serious problem if sensitive components are to be tightly packed. Kumar [20] has analyzed a feeding system similar to that suggested here. The two guides are piggybacked and coupled through small apertures, either circular holes or narrow slots oriented transversely. Applying small aperture theory, he achieves excellent experimental verification of his theoretically predicted values. The main drawback is that coupling strength never rises above -30 dB. More recently, a similar small aperture scheme was discussed by Rao *et al.* [21], extending the possible configurations to include crossed waveguide and strip and a microstrip-waveguide T-junction. All feature a coupling slot oriented transversely to the microstrip, and the same comments made on Kumar's analysis apply. As in the previous sections, coupling will occur due to beating between nondegenerate modes. In this case, we get two modes based on the dominant quasi-TEM mode in the microstrip and the TE_{10} rectangular waveguide mode. Fig. 6 shows α_{10} (E_y aligned in the two guides) and α_{11} (E_y opposed in the two guides) versus slot offset for dimensions chosen to give roughly equal propagation of the dominant modes in each guide when the slot is closed (the various parameters are listed in the figure). As is seen, α_{10} is essentially unaffected by the slot presence, while α_{11} decreases as the slot is offset. The effect of increasing the slot width $2g$ is also shown with expected larger perturbation.

Fig. 6 suggests that the α_{10} mode is closely associated with the microstrip TE_{00} mode, whereas the α_{11} mode is more aligned with the TE_{10} rectangular waveguide behavior. This is expected, if we recall that the primary coupling mechanism is the longitudinal magnetic field and the gap effect must account for the discontinuity in H_z. When the vertical electric fields are aligned (α_{10}), the gap fields are only weakly excited and the discontinuity in H_z must be small. Because the TE_{00} microstrip mode is quasi-TEM, the TE_{10}-like fields in the rectangular waveguide cannot be strongly present if the two distributions are to have approximately equal H_z components. Thus, the α_{10} mode is essentially confined to the microscrip. The α_{11} mode is the reverse. Opposition by the E_y components creates significant gap fields, and the discontinuity in H_z is most easily accounted for by a variation in the rectangular waveguide fields.

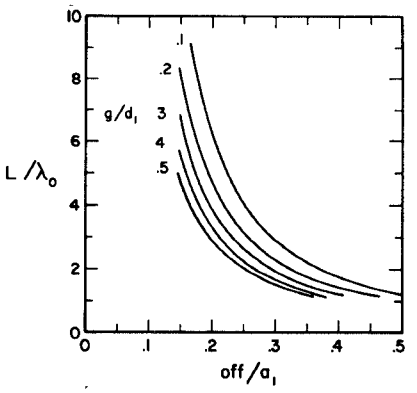

Fig. 8. Normalized coupling lengths for the parameters given in Fig. 6.

This strong reliance of the coupling mechanism on H_z is again demonstrated in Fig. 7. The same parameters are used with the gap size fixed at $g/d_1 = 0.1$, except that the microstrip permittivity is allowed to increase. Again, the offset is equal in each guide. As the permittivity increases, effectively enlarging the microstrip H_z component, the gap effect is reduced in the α_{11} mode case. As in the previous case, the α_{10} mode propagation constant is insensitive to gap changes and is essentially that of the microstrip alone. Fig. 8 shows the coupling length for the parameters used in Fig. 6. Clearly, as the slot size and offset are increased, causing α_{10} and α_{11} to differ more, the coupling length decreases. In fact, it appears that maximal power transfer can be achieved with slot lengths on the order of a free-space wavelength.

The question of how much power can be launched remains. If we ignore junction effects and simply consider the excitation of the α_{10} and α_{11} modes, then a reasonable estimate of the power coupled follows [22]. Fig. 9 shows the result of such a calculation assuming an incident rectangular waveguide TE_{10} mode of vertical electric-field magnitude $|E_2|_{in}$. The parameters are as in Fig. 6 and the slot lengths are chosen as in Fig. 8 to give maximal power

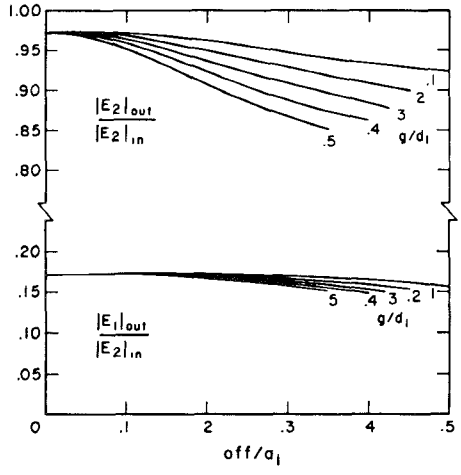

Fig. 9. Vertical electric-field transfer at maximal coupling for the parameters given in Fig. 6.

transfer. As shown, the field strength launched in the microstrip is about 15 percent of the incident value, implying that the power launched in the microstrip is roughly 17 dB down. Although hardly ideal, this compares well with the alternate approaches mentioned above. Possible slot resonances that might enhance coupling have also been ignored.

V. Discussion

The examples examined here demonstrate the manner in which the basic slot scattering problem investigated in Part I may be applied to specific waveguide structures. The strength of this approach is its flexibility to treat numerous structures. The above examples are not exhaustive. The effect of dissimilar loading in the two planar regions was largely ignored as was the possibility of placing different types of reflecting boundaries about the slot. For example, by mixing electric- and microstrip-type boundaries, one could construct rather odd waveguides, although no apparent use for these exists.

The present theory also has some simple extensions. For example, if one of the outer conductors is removed ($d_j \to \infty$), then what remains is a slotted waveguide feeding into a dielectric half-space. This type of structure may have potential remote sensing applications and has been proposed by King *et al.* [23] as a possible *in situ* dielectric measurement technique. By measuring the propagation constant of the slotted waveguide against an unknown dielectric (infinite half-space), one could determine the medium's complex permittivity by solving a modal equation similar to those developed in Part I. The difference would be that one of the $\tilde{\phi}_j$ [1, eq. (3)] would become

$$\tilde{\phi}^{(J)}(\beta_j y) = \frac{e^{-k_0 u_j y}}{u_j} \tag{7}$$

as a result of letting $d_j \to \infty$. The rest proceeds as before except that the matrices will now be 2×2. Both slotted rectangular waveguides and microstrips could be used but, because sensitivity would largely depend on the strength of the slot perturbation, the microstrip is not likely to be as useful.

A more important modification would be to allow multiple dielectric layers, like those discussed by Peng and Oliner [24], [25]. They formulate a similar transverse resource condition to determine the guidance properties in various dielectric strip and ridge guides. If the appropriate kernel for this class of structures may be found, then utilizing their reflection coefficients should lead to modal equations valid for coupling between combinations of all the above waveguide types.

At present, we have largely restricted our attention to examples of single slot coupling between two planar layers. Directly though, we could analyze multiple slot and multiple planar layers by suitably extending our basic scattering matrices. For example, by accounting for the propagation between slots, shielded-coupled microstrips could be analyzed. These shielded striplines would involve cascading our previous scattering matrices resulting in a new scattering matrix and resulting modal equation.

Alternately, multiple layers could be analyzed. For example, one could consider microstrips coupled about a central rectangular waveguide, stacked rectangular waveguides, or perhaps coupled microstrips also radiating via a slot open to free space. The scattering matrices would expand to 6×6, or 8×8, etc., but the basic formulation is the same. One need only be careful not to violate the basic assumptions needed to develop the present model.

VI. Conclusion

Part II of this paper presented four applications of the canonical slot scattering problem developed in Part I. Basically, these involved coupling between combinations of rectangular waveguides and microstrips. These examples serve to demonstrate the accuracy and limitations of the approach presented here. Additional structures featuring the same basic slot coupling are mentioned, indicating potential applications of the canonical problem presented in Part I.

References

[1] P. F. Wilson and D. C. Chang, "Mode coupling by a longitudinal slot for a class of planar waveguiding structures: Part I—Theory," *IEEE Trans. Microwave Theory Tech*, pp. 981–987, this issue.

[2] M. L. Crawford, "Generation of standard EM fields using TEM transmission cells," *IEEE Trans. Electromagn. Compat.*, vol. EMC-16, pp. 189–195, Nov. 1974.

[3] T. Chen, "Determination of the capacitance, inductance, and characteristic impedance of rectangular lines," *IEEE Trans. Microwave Theory Tech.*, vol. MTT-8, pp. 510–519, Sept. 1960.

[4] J. C. Tippet and D. C. Chang, "Characteristic impedance of a rectangular coaxial transmission line with offset inner conductor," *IEEE Trans. Microwave Theory Tech.*, vol. MTT-26, pp. 876–883, Nov. 1978.

[5] H. J. Riblet, "The characteristic impedance of a family of rectangular coaxial structures with off-centered strip inner conductors," *IEEE Trans. Microwave Theory Tech*, vol. MTT-27, pp. 294–298, Apr. 1979.

[6] J. C. Tippet, D. C. Chang, and M. L. Crawford, "An analytical and experimental determination of the cutoff frequencies of higher-order TE modes in a TEM cell," National Bureau of Standards, Boulder, NBSIR 76-841, June 1976.

[7] J. C. Tippet and D. C. Chang, "Higher-order modes in a rectangular coaxial line with thin inner conductor," National Bureau of Standards, Boulder, NBSIR 76-783, Mar. 1978.
[8] L. Gruner, "Estimating rectangular coax cutoff," *Microwave J.*, vol. 22, pp. 82–92, Apr. 1979.
[9] L. Gruner, "Characteristics of cross rectangular coaxial structures," *IEEE Trans. Microwave Theory Tech*, MTT-28, pp. 622–637, June 1980.
[10] C. M. Weil, W. T. Joines, and J. B. Kinn, "Frequency range of large scale TEM mode rectangular strip lines," *Microwave J.*, vol. 24, pp. 93–100, Nov. 1981.
[11] M. L. Crawford, J. L. Workman, and C. L. Thomas, "Expanding the bandwidth of TEM cells for EMC measurements," *IEEE Trans. Electromagn. Compat.*, vol. EMC-20, pp. 368–375, Aug. 1978.
[12] J. C. Tippet and D. C. Chang, "Dispersion and attenuation characteristics of modes in a TEM cell with lossy dielectric slab," National Bureau of Standards, Boulder, NBSIR 79-1615, Aug. 1979.
[13] D. A. Hill, "Bandwidth limitations of TEM cells due to resonances," *J. Microwave Power*, vol. 18, pp. 181–195, June 1983.
[14] E. F. Kuester, private communication.
[15] R. Levy, "Directional couplers," in *Advances in Microwaves*, L. Young, Ed., vol 1. New York: Academic Press, 1966, pp. 115–209.
[16] D. C. Chang and E. F. Kuester, "Total and partial reflection from the end of a parallel-plate waveguide with extended dielectric slab," *Radio Sci.*, vol. 16, pp. 1–13, 1981.
[17] E. F. Kuester, R. T. Johnk, and D. C. Chang, "The thin-substrate approximation for reflection from the end of a slab-loaded parallel-plate waveguide with application to microstrip patch antennas," *IEEE Trans. Antennas, Propagat.*, AP-30, pp. 910–917, Sept. 1982.
[18] R. H. Knerr, "A new type of waveguide-to-stripline transition," *IEEE Trans. Microwave Theory Tech.*, MTT-16, pp. 192–194, Mar. 1968.
[19] N. R. Wild, "Photoetched microwave transmission lines," *IEEE Trans. Microwave Theory Tech.*, vol. MTT-3, pp. 21–30, Mar. 1955.
[20] M. Kumar and B. N. Das, "Coupled transmission lines," *IEEE Trans. Microwave Theory Tech.*, vol. MTT-25, pp. 7–10, Jan. 1977.
[21] J. S. Rao, K. K. Joshi, and B. N. Das, "Analysis of small aperture coupling between rectangular waveguide and microstrip line," *IEEE Trans. Microwave Theory Tech.*, vol. MTT-29, pp. 150–154, Feb. 1981.
[22] P. F. Wilson, "On slot coupled waveguide and transmission line structures," Ph.D. thesis, University of Colorado, Boulder, May 1983.
[23] R. J. King, C. D. Kim, and J. B. Beyer, "*In situ* measurements of lossy dielectrics," Department of Electrical and Computer Engineering, University of Wisconsin, Madison, Rep. No. ECE-82-1, Jan. 1982.
[24] S. T. Peng and A. A. Oliner, "Guidance and leakage properties of a class of open dielectric waveguides: Part I—Mathematical formulations," *IEEE Trans. Microwave Theory Tech.*, vol. MTT-29, pp. 843–855, Sept. 1981.
[25] A. A. Oliner, S. T. Peng, T. I. Hsu, and A. Sanchez, "Guidance and leakage properties of a class of open dielectric waveguides: Part II —New physical effects," *IEEE Trans. Microwave Theory Tech.*, vol. MTT-29, pp. 855–869, 1981.

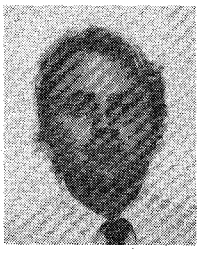

Perry F. Wilson (S'78–M'83) was born in Palo Alto, CA. He received the B. S. degree in mathematics from Stanford University in 1974, the M. S. degree in applied mathematics, and the M. S. and Ph.D. degrees in electrical engineering from the University of Colorado, Boulder, CO, in 1977, 1978, and 1983, respectively. He held a NRC Postdoctoral Research Associateship with the Electromagnetic Fields Division, National Bureau of Standards (NBS) in Boulder, CO, from July 1983 to January 1985.

Since February 1985, he has been a staff member with NBS. His technical interests include waveguides, remote sensing, and EMC/EMI related problems.

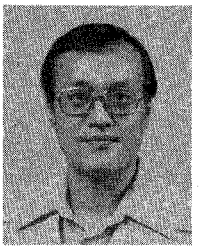

David C. Chang (M'67–SM'76–F'85) was born in Hupeh, China, on September 9, 1941. He received the B.S. degree in electrical engineering from Cheng Kung University, Tainan, Taiwan, China, in 1961, and the M.S. and Ph.D. degrees in applied physics from Harvard University, Cambridge, MA, in 1963 and 1967, respectively.

He joined the University of Colorado, Boulder, in 1967, and is now a Professor of Electrical Engineering and, since 1982, Chairman of the Electrical and Computer Engineering Department. In 1972, he was a Visiting Professor at Queen Mary College, University of London, London, England.

Dr. Chang is a member of Commission A, B, C, and E of the International Union of Radio Science, and member-at-large of its U.S. National Committee. He was an Associate Editor of IEEE TRANSACTIONS ON ANTENNAS AND PROPAGATION, the Coordinator of the IEEE/APS Distinguished Lecturer's Program, Chairman of the Subcommittee on Microwave Feilf Theory (1975–1978) of IEEE Professional Society on Microwave Theory and Techniques. He is a consultant to Kaman Science Corporation, Colorado Springs, CO., and to Teledyne micronectics, San Diego, CA.